molecular pharmaceutics

Article

pubs.acs.org/molecularpharmaceutics

Folate-Decorated and Reduction-Sensitive Micelles Assembled from Amphiphilic Polymer–Camptothecin Conjugates for Intracellular Drug Delivery

Chaoyu Liu,† Jiang Yuan,† Xiaoming Luo, Maohua Chen, Zhoujiang Chen, Yuancong Zhao, and Xiaohong Li*

Key Laboratory of Advanced Technologies of Materials, Ministry of Education of China, School of Materials Science and Engineering, Southwest Jiaotong University, Chengdu 610031, P. R. China

Supporting Information

ABSTRACT: It is one of the challenges for a wide clinical application of polymer micelles to address the structure disintegration and premature drug release before reaching a pathological site. In the current study, folic acid (FA)-decorated polymer–drug conjugates (FSC) were synthesized with disulfide linkages between camptothecin (CPT) and amphiphilic poly(ethylene glycol)-*b*-poly(*ε*-caprolactone) (PECL) copolymers. FSC conjugates were proposed to assemble into micelles with a hydrophobic core of PCL segments and CPT and a hydrophilic corona of PEG segments. The addition of hexadecanol during micelle formation (FSC-16) was proposed to modulate the interactions of hydrophobic segments in micelles and enhance the reductive sensitivity. FSC-16 micelles were obtained with critical micelle concentration of around 2 *μ*g/mL and an average size of around 200 nm, and the conjugated CPT was rapidly released out in response to glutathione. The reductive sensitivity was also demonstrated with respect to the changes of micelle size and morphologies as well as the fluorescent intensity of pyrene loaded in micelles. Benefiting from the FA receptor-mediated uptake and the reduction-sensitive release of CPT, significant cytotoxicity and cell apoptosis were identified for FSC-16 micelles against SKOV-3 cells with strong expressions of FA receptors. Flow cytometry and confocal laser scanning microscopy analyses demonstrated that CPT was distributed into nuclei after cellular uptake and intracellular release from FSC-16 micelles. Thus, the FA-decorated and reduction-sensitive micelles assembled from polymer–drug conjugates show advantages in inhibiting premature release during circulation, enhancing cellular uptake at the tumor tissues, and promoting intracellular release and nuclei location of the active moieties.

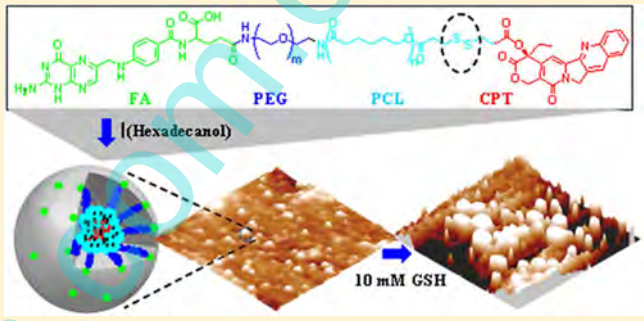

KEYWORDS: *polymer–drug conjugate micelle, disulfide linkage, folic acid decoration, reductive sensitivity, nucleus localization*

INTRODUCTION

During the past decade, nanomedicine has emerged as an effective strategy for target delivery and controlled release of drugs, genes, and imaging agents. The nanoscale formulations include liposomes, polymeric micelles, and nanoparticles. Micelles self-assembled from amphiphilic copolymers have become one of the most promising carriers of anticancer drugs, manifesting several attractive features such as the core–shell structure to effectively protect and enhance the water solubility of anticancer drugs in the core. Additionally, the hydrophilic coronas and size distributions of polymeric micelles alleviate the phagocytic and renal clearance to achieve a prolonged circulation time, a decrease in the systemic side effects, and a passive accumulation into tumor tissues by the enhanced permeability and retention (EPR) effect.[1] Polymeric micelles with loaded paclitaxel (Genexol-PM) and doxorubicin (NK911) have already been evaluated clinically in several countries.[2]

However, there are several challenges that need to be addressed for a wide clinical application of polymeric micelles. The conventional biodegradable micelles based on hydrophilic segments, such as poly(ethylene glycol) (PEG) and poly(amino acid), and aliphatic polyesters, such as polylactide (PLA) and poly(*ε*-caprolactone) (PCL), usually show sustained degradation kinetics inside the body over a period of days to weeks, leading to reduced drug efficacy and even drug resistance.[3,4] In this regard, stimuli-responsive biodegradable micelles have been explored extensively in recent years, and the stimuli signals included pH, temperature, ultrasound, enzyme, and reduction environment.[5] Stimulus-sensitive micelles that encapsulated hydrophobic drugs indicated significant and rapid changes in

Received: July 6, 2014
Revised: August 18, 2014
Accepted: September 19, 2014
Published: September 19, 2014

dx.doi.org/10.1021/mp500468d | *Mol. Pharmaceutics* 2014, 11, 4258–4269

their physicochemical properties such as the morphology and solubility, eventually leading to selectively enhance the drug release at the target site in response to an internal or external stimulus.[6] Particularly, reduction-sensitive micelles that contained disulfide linkages have received much more interest for intracellular drug delivery because of a specific degradation in response to redox potential through a thiol−disulfide exchange reaction.[6] Inside the body, glutathione (GSH), a natural reducing agent for disulfide bonds, was found in human blood at μM levels, whereas a substantially high concentration at mM levels was found in the cytoplasm. Additionally, GSH metabolism is possibly associated with cancer development and drug resistance, and the GSH concentration in cancer cells was found to be several times higher than that in normal cells.[7] Taking use of these different levels of GSH, the disulfide-linked micelles could keep stable during circulation and in the extracellular environment, but exhibit rapid intracellular drug release after cellular uptake.[4] Up to now shell-sheddable micelles have been widely examined from amphiphilic copolymers with disulfide bonds between the hydrophobic and hydrophilic blocks.[8] However, micelles containing reduction-cleavable linkages positioned in the chains of hydrophobic blocks were rarely reported yet.

Another challenge is the premature release of drug due to the disintegration of polymeric micelles during circulation in blood before reaching a pathological site, although it is believed to be more stable than liposomes and emulsions constructed from conventional surfactants.[9] The high dilution, ionic strength, large shear forces, and the presence of numerous charged blood components can affect the micelle stability, which is the main reason for the side effects and dramatic decreases in the therapeutic efficacy.[10] To solve these problems, one of the strategies is to cross-link either the core or shell of polymeric micelles through bifunctional reagents, free radical polymerization, photo-cross-linking, or stimuli-responsive linkers.[11] Bütün et al. prepared triblock copolymers to form micelles containing PEG outer coronas, cross-linkable middle shells, and hydrophobic cores. The cross-linked shell held the micelle nanostructure during circulation and avoided burst release in the initial stage.[12] To accelerate drug release in the cytoplasm, Wang et al. synthesized a triblock copolymer poly(ethylene glycol)-*b*-poly(L-lysine)-*b*-poly(rac-leucine), in which PEG segments were attached with poly(L-lysine) blocks via disulfide linkages, and the shell was cross-linked using disulfide-containing cross-linkers. In the presence of GSH, the micelles underwent destruction of the cross-linked shell, removal of the PEG corona, and collapse of the micelles, leading to a dramatic acceleration of drug release at a cytoplasmic GSH level.[13] Another strategy to alleviate the premature release is proposed recently through chemical conjugation of hydrophobic anticancer drug onto polymers, and the amphiphilic prodrugs are self-assembled into stable micelles. Compared with micelles with drug loadings via physical entrapment, polymer−drug conjugate micelles indicate more advantages such as enhanced drug stability and intracellular uptake and alleviate burst release at the early stage.[14]

Camptothecin (CPT) is a potent broad-spectrum anticancer drug, but the poor aqueous solubility, high systemic toxicity, and rapid pH-dependent hydrolysis of the lactone ring into an inactive carboxylate form have severely restricted its clinical application.[15] One effective approach to overcome these drawbacks is to convert into CPT prodrugs to enhance water solubility, which can change back to the active moiety triggered by unique environmental stimuli.[16] An additional advantage of such conjugates is the ability to stabilize the lactone structure after conjugation with the hydroxyl group of CPT.[17] Zhang et al. prepared azide-functionalized CPT derivatives, followed by conjugation with poly(aspartic acid) derivative containing alkyne groups by click cycloaddition to give drug-conjugated micelles, indicating a continuous low dose release due to the relatively stable linkers.[18] To accelerate the drug release from micelles, Fan et al. prepared disulfide-linked poly(amido amine) containing alkyne groups, followed by conjugation with azide-functionalized CPT, indicating around 40% of accumulated release after 2 weeks due to the breakage of disulfide linkages in the polymer backbone. However, the hydrolysis of ester bonds between CPT and polymer backbone led to a much slower release of active CPT than the polymer degradation.[19] Alternatively, Li et al. prepared PEG−CPT conjugates with disulfide linkages between them to self-assemble into micelles. However, a relatively high critical micelle concentration (CMC) of 60 μg/mL and large initial burst release were determined, due to the less optimal balance between the hydrophilic and hydrophobic segments.[20]

In the current study, novel reduction-sensitive biodegradable micelles were designed from folic acid (FA)-decorated amphiphilic polymer−CPT conjugates with disulfide linkages (FSC). The inoculation of disulfide linkers between CPT and amphiphilic poly(ethylene glycol)-*b*-poly(ε-caprolactone) (PECL) copolymers was supposed to release the active CPT in responsive to intracellular GSH. FA has been popularly employed as a targeting moiety of various anticancer agents to avoid nonspecific attacks on normal tissues as well as to increase their cellular uptake within target cells.[21] The addition of hexadecanol into FSC micelles was proposed to modulate the interactions of hydrophobic segments and CPT release profiles. The reductive sensitivity was evaluated with respect to the changes of micelle sizes and morphologies as well as the fluorescent intensity of pyrene loaded in micelles after incubation with different GSH levels. The FA receptor-mediated cellular uptake, intracellular drug release, cytotoxicity, and apoptosis induction of drug-conjugated micelles were investigated against tumor cells with different expression profiles of FA receptors.

EXPERIMENTAL SECTION

Materials. 3,3′-Dithiodipropionic acid (DTPA), stannous chloride, *N*,*N*-dicyclohexylcarbodiimide (DCC), *N*-hydroxysuccinimide (NHS), di-*tert*-butyl dicarbonate ($(Boc)_2O$), PEG (M_w = 2 kDa), FA, GSH, and 4-dimethylamino-pyridine (DMAP) were used as received from Aladdin (Beijing, China). CPT was from Knowshine Pharmachemicals Inc. (Shanghai, China), and ε-caprolactone (ε-CL) was procured from Alfa Aesar (Ward Hill, MA). 3-(4,5-Dimethylthiazol-2-yl)-2,5-diphenyltetrazolium bromide (MTT), propidium iodide (PI), and dialysis membrane (1 kDa cutoff) were obtained from Sigma-Aldrich (St. Louis, MO). All other chemicals were analytical grade and obtained from Changzheng Regents Company (Chengdu, China), unless otherwise indicated. Dimethyl sulfoxide (DMSO), *N*,*N*-dimethylformamide (DMF), and pyridine were dried over CaH_2 and distilled under reduced pressure prior to use. Dichloromethane (DCM) and triethylamine were dried with 4 Å molecular sieves and redistilled before use. Acetyl chloride and methanesulfonyl chloride (MsCl) were refluxed with PCl_5 and P_2O_5, respectively, followed by distillation under reduced pressure.

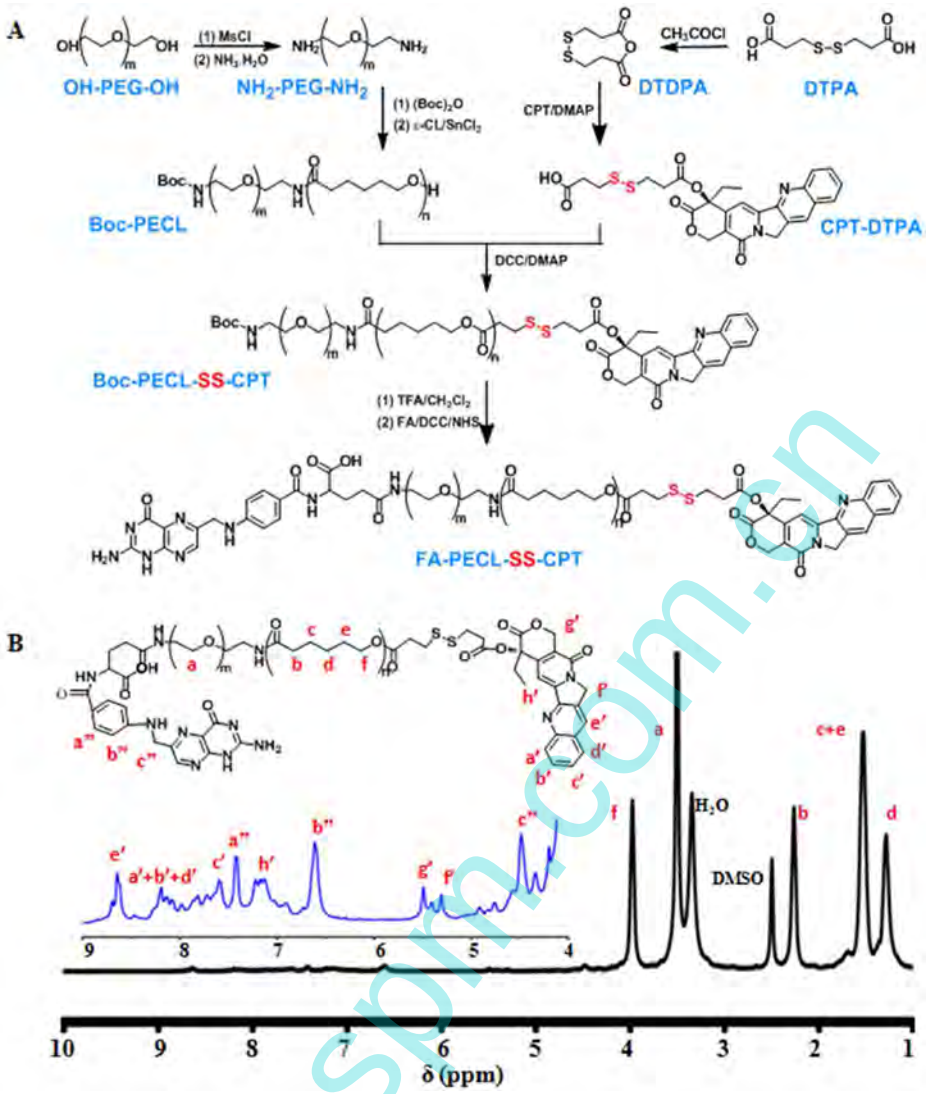

Figure 1. (A) Synthesis route and (B) ^{1}H NMR spectrum of FA-decorated polymer−drug conjugates containing disulfide linkages between CPT and amphiphilic PECL copolymers (FA-PECL-SS-CPT, FSC).

Synthesis of FSC Polymer−Drug Conjugates. The synthesis routes of FSC polymer−drug conjugates are outlined in Figure 1A. For comparison, FA-decorated amphiphilic polymer−CPT conjugates without disulfide linkage (FC) was also prepared (Figure S1A, Supporting Information). The molecular weights and block compositions of the copolymers were estimated from ^{1}H NMR spectra recorded on a 400 MHz Bruker spectrometer (Billerica, MA) using deuterated chloroform ($CDCl_3$) or deuterated dimethyl sulfoxide (DMSO-d_6) as solvent. Fourier transform infrared (FTIR) spectra were recorded on a Nicolet 5700 spectrometer (Thermo Electron, USA). The molecular weight and polydispersity index of polymers were measured by gel permeation chromatography (GPC, waters 2695 and 2414, Milford, MA) using tetrahydrofuran as the eluent at a flow rate of 1.0 mL/min.

Synthesis of *N-tert*-Butoxycarbonyl-Protected PECL Copolymers. *N-tert*-Butoxycarbonyl (N-Boc) protected PECL copolymers (Boc-PECL) were synthesized through ring-opening polymerization of ε-CL with N-Boc-protected PEG diamine (Boc-PEG-NH_2). PEG diamine was prepared as previously described with some modifications.[22] Briefly, PEG (3.00 g, 1.5 mmol) was dissolved in anhydrous DCM (44 mL), followed by the addition of triethylamine (4.94 mL, 17.6 mmol). After adding MsCl (0.7 mL, 4.41 mmol) dropwise under argon stream, the reaction proceeded overnight at room temperature, and the product was precipitated with ethyl ether and vacuum-dried to give PEG-mesylate. The mesylated PEG was mixed with 25 wt % ammonia aqueous solution in an autoclave, and the reaction continued at 120 °C for 10 h. The mixture was extracted with DCM, followed by back-extraction with saturated sodium chloride solution. Then, the product was precipitated with excess ethyl ether and vacuum-dried to give PEG diamine. Yield = 49%. ^{1}H NMR ($CDCl_3$, ppm): δ 3.64 ($-CH_2CH_2-O-$), 2.93 ($-CH_2-NH_2$), and 2.12 ($-NH_2$) (Figure S2A, Supporting Information).

A dioxane solution of $(Boc)_2O$ (0.50 g, 2.3 mmol) was added dropwise to PEG diamine (4.60 g, 2.3 mmol) in 20 mL of $NaHCO_3$ (0.1 M) aqueous solution, and the resulting solution was stirred at room temperature overnight. Then, the pH of the solution was adjusted to 8.0 by dilute HCl. After filtration the solution was evaporated, dissolved in DCM, precipitated with excess ethyl ether, and vacuum-dried to give Boc-PEG-NH_2. Yield = 83%. FTIR (KBr pellet): 1701 cm^{-1} (amide). Copolymer Boc-PECL was prepared by ring-opening polymer-

ization of ε-CL (1.86 g, 16.3 mmol) at 140 °C using Boc-PEG-NH_2 (0.80 g, 0.4 mmol) as an initiator and stannous chloride (0.03 g, 0.14 mmol) as a catalyst. The resulting polymer was precipitated with excess ethyl ether and vacuum-dried. Yield = 90%. ^{1}H NMR ($CDCl_3$, ppm): δ 4.06 (−CH_2−O−), 3.75 (−CH_2CH_2−O−), 2.31 (−C(=O)−CH_2−), 1.65 (−CH_2−), 1.38 (−CH_2−), 1.24 (−$C(CH_3)_3$) (Figure S2B, Supporting Information).

Synthesis of Disulfide-Linked Carboxyl-Terminal CPT and Succinyloxide-Modified CPT. Disulfide-linked carboxyl-terminal CPT (CPT-ss-COOH) was synthesized from esterification of CPT with dithiodipropionic anhydride (DTDPA), which was obtained by acylation of DTPA with acetyl chloride. Briefly, DTPA (2 g, 9.6 mmol) was dissolved in acetyl chloride (15 mL) and refluxed at 65 °C for 5 h. After solvent removal, the residue was precipitated into excess ethyl ether to afford DTDPA and vacuum-dried. To a dry pyridine solution (35 mL) of DTDPA (2.35 g, 12.9 mmol) and CPT (0.450 g, 1.29 mmol), a solution of DMAP (0.631, 5.17 mmol) in 10 mL of pyridine was added dropwise at 0 °C under argon atmosphere. The resulting mixture was heated to 70 °C, and the reaction proceeded for 48 h. Then, the reaction solution was precipitated into excess methanol, washed with dilute HCl, and vacuum-dried to give CPT-ss-COOH. Yield = 52%. ^{1}H NMR (DMSO-d_6, ppm): δ 12.35 (d, 1H, −COOH), 8.69 (s, 1H, =CH−), 8.12−8.17 (m, 2H, =CH−), 7.87 (t, 1H, =CH−), 7.72 (t, 1H, =CH−), 7.18 (s, 1H, =CH−), 5.50 (s, 2H, −O−CH_2−), 5.30 (s, 2H, -N−CH_2−), 2.99−3.13 (m, 2H, −CH_2−CH_3), 2.95 (m, 2H, −CH_2−SS-CH_2−), 2.61 (m, 10H, −S−CH_2−COO−), 2.16 (m, 2H, −S−CH_2−COOH), 0.93 (m, 3H, −CH_3) (Figure S3B, Supporting Information).

Succinyloxide-modified CPT was prepared as above using succinic anhydride (3.45 g, 34.5 mmol) instead of DTDPA to give CPT-COOH. Yield = 90%. ^{1}H NMR (DMSO-d_6, ppm): δ 12.25 (d, 1H, −COOH), 8.69 (s, 1H, =CH−), 8.11−8.19 (m, 2H, =CH−), 7.87 (t, 1H, =CH−), 7.72 (t, 1H, =CH−), 7.13 (s, 1H, =CH−), 5.49 (s, 2H, −O−CH_2−), 5.28 (s, 2H, -N−CH_2−), 2.75 (m, 2H, −CH_2−CH_3), 2.46 (m, 2H, −CH_2−COOH), 2.15 (m, 2H, −CH_2−COO−), 2.16 (m, 2H, −S−CH_2−COOH), 0.92 (m, 3H, −CH_3) (Figure S3C, Supporting Information).

Synthesis of Boc-PECL-ss-CPT and Boc-PECL-CPT Conjugates. Boc-PECL-ss-CPT and Boc-PECL-CPT conjugates were synthesized by coupling Boc-PECL with CPT-ss-COOH and CPT-COOH, respectively. Briefly, Boc-PECL (0.672 g, 0.076 mmol) in anhydrous DMF (10 mL) was added dropwise to an anhydrous DMF solution (20 mL) of excess CPT-ss-COOH (0.121 g, 0.224 mmol), DCC (0.120 g, 1.04 mmol), and DMAP (0.050 g, 1.45 mmol) at 0 °C under argon atmosphere. The resulting solution was warmed to 30 °C and the reaction continued for 48 h. Then, the mixture was distilled under reduced pressure, precipitated with excess ethyl ether and vacuum-dried to give Boc-PECL-ss-CPT. Yield =80%. ^{1}H NMR (DMSO-d_6, ppm): δ 8.70 (=CH−), 8.19 (=CH−), 7.86 (=CH−), 7.72 (=CH−), 7.17 (=CH−), 5.50 (−O−CH_2−), 5.31 (-N−CH_2−), 3.98 (−O−CH_2−), 3.51 (−CH_2CH_2−O−), 2.93 (−CH_2−SS-CH_2−), 2.67 (-S-CH2-COO−), 2.27 (-C(=O)−CH_2−), 1.53 (−CH_2−), 1.29 (−CH_2−), 1.03 (−$C(CH_3)_3$), 0.93 (−CH_3) (Figure S4A, Supporting Information).

Conjugation of FA onto PECL-ss-CPT and PECL-CPT. Polymer−drug conjugates FSC and FC were synthesized by reaction of activated FA with deprotected PECL-ss-CPT and PECL-CPT, respectively. Briefly, to remove the *tert*-butoxycarbonyl (*t*-BOC) groups, Boc-PECL-ss-CPT (0.800 g) in anhydrous DCM (10 mL) was added dropwise to trifluoroacetic acid (3 mL) at room temperature. After stirring for 12 h, the solution was evaporated, precipitated with ethyl ether, and vacuum-dried to give NH_2-PECL-ss-CPT. The carboxyl group of FA was activated by incubation with FA (0.500 g), NHS (0.272 g), and DCC (0.468 g) in anhydrous DMSO (10 mL) at room temperature under argon for 12 h. The solution was filtered and directly reacted with NH_2-PECL-ss-CPT (0.800 g, 0.09 mmol) in 18 mL of anhydrous DMSO, followed by the addition of triethylamine (2.0 mL, 7.13 mmol). After stirring under argon at room temperature for 12 h, the solution was purified by dialysis against DMSO for 24 h and water for 48 h, followed by lyophilization to give FSC. Yield = 70%. FC was synthesized following the same procedures as above. Yield = 75%. ^{1}H NMR (DMSO-d_6, ppm): δ 8.62 (=CH−), 8.21 (=CH−), 7.84 (=CH−), 7.70 (=CH−), 7.42 (=CH−CO−), 7.21 (=CH−), 6.60 (=CH−N−), 5.50 (−O−CH_2−), 5.31 (−N−CH_2−), 4.50 (−N−CH_2−), 3.98 (−O−CH_2−), 3.51 (−CH_2CH_2−O−), 2.27(−C(=O)−CH_2−), 1.53 (−CH_2−), 1.31 (−CH_2−), 0.93 (−CH_3) (Figure S1B, Supporting Information).

Preparation and Characterization of Micelles. Polymeric micelles were prepared from FSC and FC conjugates by a solvent evaporation method as described previously.[23] Briefly, 5 mg of FSC or FC was dissolved in 20 mL of THF and added dropwise into 10 mL of deionized water under vigorous stirring. The resulting suspension was kept under stirring overnight to remove THF to form FSC or FC micelles. Additionally, hexadecanol (0.75 mg) and 5 mg of FSC (or FC) conjugates was dissolved in THF, and FSC-16 (or FC-16) micelles were prepared following the same procedures.

The CMC of micelles was determined by fluorescence spectroscopy using the pyrene probe as described previously.[24] The concentration of the micelles varied from 4×10^{-5} to 0.5 M, while the final concentration of pyrene was set to be 0.6 μM. The fluorescence intensity at the emission wavelengths of 390 nm was recorded by a fluorescence spectrophotometer (Hitachi F-7000, Japan), and the CMC was estimated by the ratios of fluorescence intensities at 339 and 333 nm of exciting wavelengths. The average size, size distribution, and zeta potential of micelles were detected by dynamic light scattering (DLS, Nano-ZS90, Malvern Ltd., U.K.). The morphology of micelles was tested using transmission electron microscopy (TEM, JEM-2100F, JEOL, Tokyo, Japan) operated at an accelerating voltage of 200 kV and atomic force microscopy (AFM, CSPM5000, Being, China) with the tapping mode. Thermal analysis of FSC micelles was recorded by differential scanning calorimeter (DSC, Q20, TA Instruments, New Castle, DE) at a heating rate of 10 °C/min and a temperature range of 0−270 °C.

Reductive Sensitivity of Micelles. The reductive sensitivity of micelles was estimated from CPT release profiles as well as the changes of micelle sizes and morphologies after incubation in phosphate buffered saline (PBS, pH 7.4) containing 2 μM and 10 and 40 mM GSH. Briefly, micelle suspensions were placed in dialysis bags (1 kDa cutoff), immersed into 30 mL of release media to achieve a sink condition, and kept shaking at 37 °C and 100 cycles/min. At given time intervals, 1.0 mL of release media was withdrawn and refreshed with PBS containing GSH. The release media were detected by fluorospectrophotometer at the excitation

wavelength of 380 nm and the emission wavelength of 550 nm, in which CPT content was obtained using a standard curve from known concentrations of CPT solutions. In another batch of micelle incubation, micelles were retrieved for size measurement by DLS and morphological observation by AFM. The reductive sensitivity was also determined by fluorescence intensities of pyrene loaded in micelles after treatment with GSH.[25] Briefly, micelles were incubated into PBS containing 2 μM and 10 and 40 mM GSH, and pyrene was loaded with the final concentration of 0.6 μM. After incubation at 37 °C as above, the fluorescent spectra of pyrene in micelles were recorded at the emission wavelength of 390 nm.

***In Vitro* Cytotoxicity of Micelles.** The *in vitro* cytotoxicity of micelles was evaluated by MTT assay on FA receptor-negative human lung adenocarcinoma cells A549, FA receptor-positive human breast carcinoma cells MCF-7, and human ovarian carcinoma cells SKOV-3 (American Type Culture Collection, Rockville, MD). Briefly, A549 cells were cultured in FA-free RPMI-1640 (Gibco BRL, Rockville, MD) containing 10% fetal bovine serum (FBS, Gibco BRL, Rockville, MD), while MCF-7 and SKOV-3 cells were maintained in FA-free DMEM (Gibco BRL, Rockville, MD) containing 10% FBS. Cells were seeded into 96-well tissue culture plates (TCP) at a density of 3000 cells/well in 100 μL of medium and incubated for 24 h. Then, the cells were cultured in media containing free CPT, FSC, FSC-16, and FC-16 micelles with final CPT concentrations from 10 ng/mL to 10 μg/mL. For comparison, media containing 10 μg/mL FA were used in the tests on FSC-16 micelles, and cells without treatment were used as control. After incubation for 72 h, the cell viability was determined by MTT assay as described previously.[26]

Cellular Uptake of Micelles. The cellular uptake and intracellular CPT release profile of micelles were estimated by flow cytometry and confocal laser scanning microscopy (CLSM). Briefly, A549 and SKOV-3 cells were seeded into 6-well TCP at a density of 1×10^6 cells/well and incubated for 24 h. The cells were cultured in media containing free CPT, FSC-16, and FC-16 micelles with a final CPT concentration of 10.0 μg/mL. For comparison, media containing 10 μg/mL FA were used in the tests on FSC-16 micelles, and cells without treatment were used as control. After incubation for 6 h, cells were washed with PBS three times, harvested by trypsin digestion, and fixed with 4% formaldehyde. Then, the cells were collected by centrifugation and resuspended in PBS, followed by analysis of the cell suspensions by flow cytometry (BD Accuri C6, Franklin Lakes, NJ). The data was analyzed using WinMDI 2.9 software. In another batch of experiment, SKOV-3 cells were washed twice with PBS, fixed with 4% formaldehyde solution, and stained with PI for 30 min, followed by CLSM observation.

***In Vitro* Cell Apoptosis Induced by Micelles.** The cell apoptosis was quantified by an Annexin V-fluorescein isothiocyanate (FITC) apoptosis detection kit (Beijing 4A Biotech Co., Beijing, China) according to the manufacturer's instructions. Briefly, SKOV-3 cells were seeded in culture dishes and allowed to attach overnight, followed by exposure to different micelles for 48 h. The attached and floating cells were harvested with 0.25% trypsin, washed twice with PBS, and suspended in 500 μL of binding buffer. After the addition of 5 μL of Annexin V-FITC and 5 μL of PI, the samples were gently mixed and incubated at room temperature for 15 min before analysis with flow cytometry. Data analysis was performed using BD FACSuite (BD Biosciences, CA).

Statistics Analysis. Data are expressed as mean ± standard deviation (SD). The statistical significance of the data obtained was analyzed by the Student's *t* test. Probability values of $p < 0.05$ were interpreted as denoting statistical significance.

RESULTS AND DISCUSSION

Characterization of Polymer–Drug Conjugates. Because of the poor aqueous solubility and instability of the lactone ring, CPT has received much attention in the field of drug delivery systems to improve the *in vivo* stability and therapeutic efficacy.[27] In the current study, we synthesized an amphiphilic polymer–drug conjugate FSC containing FA at the hydrophilic end and disulfide linkage between PECL copolymer and CPT (Figure 1A). PECL is one kind of widely used biodegradable amphiphilic copolymer in drug delivery systems with the characteristic of core–shell geometry in micelles.[28] As shown in Figure 1A, copolymer Boc-PECL was prepared by ring-opening polymerization of ε-CL using Boc-PEG-NH_2 as a macroinitiator. The amount of amino groups was determined by the ninhydrin method,[29] indicating that the amino concentration of Boc-PEG-NH_2 decreased by 52.2% compared to that of PEG diamine. The molecular weight of PEG diamine was 1790, determined from the ^{1}H NMR spectrum (Figure S2A, Supporting Information), which agreed with 1619 of M_n determined from of GPC measurement with M_w/M_n of 1.06. The molecular weight of Boc-PECL was 8800, estimated from the ^{1}H NMR spectrum (Figure S2B, Supporting Information) by comparing the peak integration of methylene protons of PCL blocks ($-C(=O)CH_2CH_2-$, δ = 2.31 ppm) to that of PEG blocks ($-CH_2CH_2O-$, δ = 3.64 ppm).

DTPA, as a stable disulfide-containing reagent, can be conveniently transformed into DTDPA through dehydration reaction, which is effective to conjugate with hydroxyl groups of CPT.[30] Additionally, β-thioester bonds formed as the linker between DTPA and CPT are easily hydrolyzed to release the active moiety by esterase, which is abundant in cells.[31] As shown in Figure 1A, the terminal hydroxyl group of CPT was coupled with anhydride group of DTDPA by esterification using DMAP as a catalyst to produce an intermediate, CPT-ss-COOH. Compared with those of CPT (Figure S3A, Supporting Information), additional peaks at 2.61, 2.95, 2.16, and 12.35 ppm in the ^{1}H NMR spectrum of CPT-ss-COOH (Figure S3C, Supporting Information) belonged to protons of $-S-C-CH_2-C(=O)O-$, $-CH_2-SS-CH_2-$, $-OC(=O)CH_2C-S-$, and $HOC(=O)-$, respectively, and the peaks at 2.15, 2.46, and 12.25 ppm were assigned to protons of $-C-CH_2-C(=O)O-$, $-(O=)C-CH_2C-C(=O)-$, and $HOC(=O)-$ of CPT-COOH, respectively (Figure S3B, Supporting Information). The peak at 5.28 ppm (−C−OH in CPT) disappeared completely in ^{1}H NMR spectra of CPT-ss-COOH and CPT-COOH, indicating an almost complete esterification of hydroxyl groups of CPT.

FA receptors are overexpressed on epithelial tumors of various organs, such as brain, kidney, breast, and lung, but rarely expressed in normal tissues.[21] FA-conjugated biodegradable micelles and nanoparticles have been investigated and delivered into cancer cells via receptor-mediated endocytosis.[32] As shown in Figure 1A, Boc-PECL-ss-CPT was synthesized by coupling the terminal hydroxyl groups of Boc-PECL with DCC-activated carboxyl groups of CPT-ss-COOH, followed by treatment with trifluoroacetic acid to remove *t*-Boc groups to give NH_2-PECL-ss-CPT. Compared with the ^{1}H NMR spectrum of Boc-PECL-ss-CPT (Figure S4A, Supporting

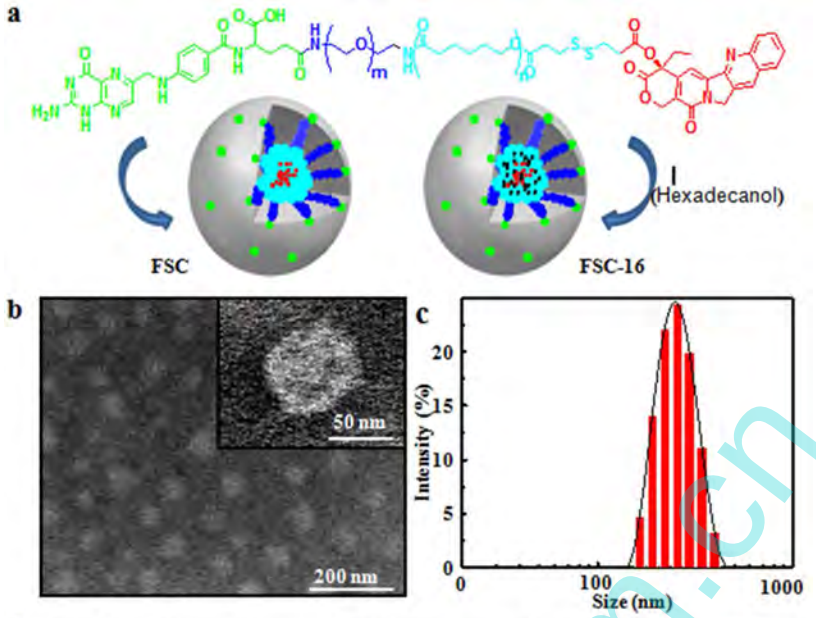

d

Sample	Average size (nm)	Polydispersity index	Zeta potential (mV)	CMC (μg/mL)
FSC	180	0.416	-21.3	2.2
FSC-16	196	0.135	-20.6	1.8
FC	155	0.512	-24.3	2.4
FC-16	185	0.354	-21.1	1.5

Figure 2. (a) Illustration of the formation of FSC micelles, and hexadecanol was added to modulate the interactions of hydrophobic segments in micelles. (b) Typical TEM and (c) DLS images showing the morphology and size distribution of FSC-16 micelles. (d) Summary of the average sizes and the polydispersity indices, the zeta potentials, and CMC values of FC, FC-16, FSC, and FSC-16 micelles.

Information), the peak at 1.03 ppm ($-C(CH_3)_3$ in *t*-Boc group) almost disappeared for NH_2-PECL-ss-CPT (Figure S4B, Supporting Information). Subsequently, FA was activated by DCC/NHS protocol and reacted with the terminal amino group of NH_2-PECL-ss-CPT, forming an amide bond. Figure 1B shows the ^1H NMR spectrum (DMSO-d_6, ppm) of FSC as well as detailed assignment of each peak: δ 8.65 (=CH−), 8.19 (=CH−), 7.82 (=CH−), 7.72 (=CH−), 7.42 (=CH−CO−), 7.22 (=CH−), 6.61 (=CH−N−), 5.49 ($-O-CH_2-$), 5.31 ($-N-CH_2-$), 4.48 ($-N-CH_2-$), 3.98 ($-O-CH_2-$), 3.50 ($-CH_2CH_2-O-$), 2.92 ($-CH_2-SS-CH_2-$), 2.67 ($-S-CH_2-COO-$), 2.27($-C(=O)-CH_2-$), 1.54 ($-CH_2-$), 1.29 ($-CH_2-$), 0.93 ($-CH_3$). Compared with that of NH_2-PECL-ss-CPT (Figure S4B, Supporting Information), additional peaks at 7.42, 6.61, and 4.48 ppm belonged to protons of methene in the benzene ring, indicating the presence of FA groups.

Characterization of Drug-Conjugated Micelles. Figure 2a illustrates the formation of FSC and FSC-16 micelles, and hexadecanol was added to modulate the interaction of hydrophobic segments in micelles. To identify the micelle formation, FSC micelles were evaluated by ^1H NMR in D_2O. As shown in Figure S5, Supporting Information, in comparison with the spectrum of FSC conjugates in DMSO-d_6, signals from protons of PCL segments and CPT were absent in the spectrum of FSC micelles in D_2O except for that of PEG segments and FA. It was suggested the conjugates tend to self-assemble into a core−shell micellar structure with a hydrophobic core of PCL segments and CPT and a hydrophilic shell of PEG segments.[33] Figure 2b shows a typical TEM image of FSC-16 micelles, indicating a spherical morphology with an average size of around 60 nm. Figure 2c shows the size distribution of FSC-16 micelles, indicating an average size of around 200 nm measured through DLS. It should be noted that the small size observed from TEM images was due to the volume shrinkage of micelles during the drying process of samples. The pore cutoff size of blood vessels in most tumors is known to be 380−780 nm.[34] Thus, the size ranges of micelles obtained, along with the hydrophilic corona, makes them ideal drug delivery carriers for vascular permeability and escaping from renal exclusion and the reticuloendothelial system.[35] As shown in Figure 2d, the zeta potentials of all these micelles were over −20 mV, suggesting strong repellent forces among micelles to achieve a good stability.[36] The CMCs of these micelles were determined using pyrene as a fluorescent probe. Figure S6, Supporting Information, shows the plots of fluorescence intensity ratios I_{339}/I_{333} of pyrene versus polymer concentrations, and Figure 2d summarizes the results. The CMC values of FSC-16 (ca. 1.8 μg/mL) and FC-16 micelles (ca. 1.5 μg/mL) after hexadecanol inoculation were lower than those of FSC (ca. 2.2 μg/mL) and FC micelles (ca. 2.4 μg/mL), respectively. It should be noted that FSC-16 micelles indicated over 10-fold lower CMC after insertion of PCL segments between PEG and CPT, compared with PEG-CPT conjugate micelles with or without disulfide linkages.[20,31]

***In Vitro* Reduction-Sensitive Release of CPT from Micelles.** Disulfide linkages between the matrix polymer and CPT can be readily broken in the presence of reducing agents. To examine the responsiveness, the CPT release from FSC and

FSC-16 micelles was investigated in the presence or absence of GSH and compared with those of FC and FC-16 micelles. GSH concentrations of 2 μM and 10 and 40 mM were used to represent the reductive microenvironment of extracellular space and cytoplasm of normal and tumor cells, respectively.[7,37] As illustrated in Figure 3a, less than 10% of CPT release from FC micelles after incubation in the absence of GSH and with 10 mM GSH for 100 h, due to the hydrolysis of ester bonds between CPT and the backbone. The CPT release from FSC micelles after incubation with 2 μM GSH for 100 h was below 10%, similar to that in the absence of GSH. However, a significantly higher amount of CPT release at around 38% was detected for FSC micelles after incubation with 10 mM GSH for 100 h ($p < 0.05$), indicating the reductive sensitivity of CPT release. The increase of GSH concentration to 40 mM led to a significantly higher CPT release from FSC micelles ($p < 0.05$), at about 53% after incubation for 100 h.

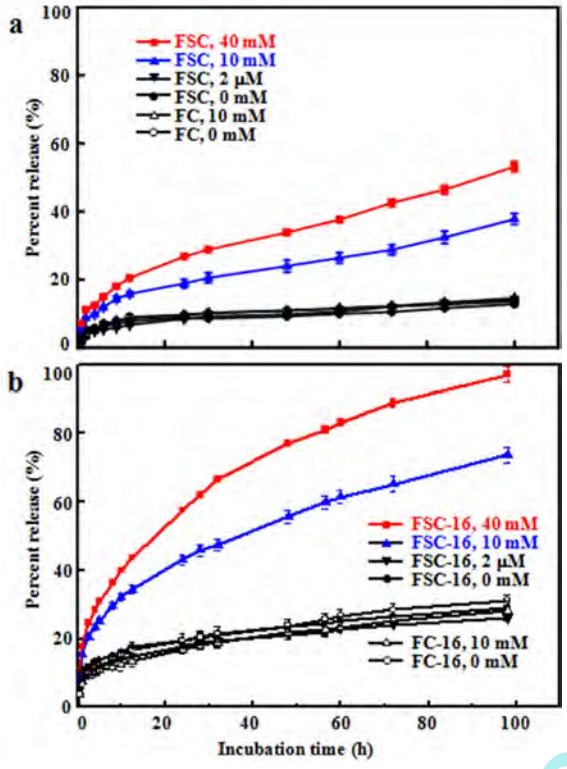

Figure 3. Percent release of CPT from (a) FSC and (b) FSC-16 micelles after incubation at 37 °C in PBS and PBS containing 2 μM and 10 and 40 mM GSH, compared with FC and FC-16 micelles without disulfide linkage (n = 3).

It should be noted that the CPT release was lower compared with micelles with physical entrapment of anticancer drugs,[38] due to the embedment of disulfide linkages in highly arranged PCL segments during micelle formation. An effective concentration of anticancer drugs is often essential to obtain aggressive activity within tumor cells for an enhanced therapeutic efficacy.[39] To disrupt the arrangement of PCL segments in micelles, hexadecanol was included during micelle preparation. To demonstrate possible interactions among the copolymer, CPT, and hexadecanol, DSC analysis of freeze-dried FSC and FSC-16 micelles was carried out. As shown in Figure S7, Supporting Information, CPT showed two endothermic melting peaks at 247.5 and 266.3 °C. However, no endothermic peak of CPT was present in FSC and FSC-16 micelles, indicating a low crystallinity of CPT in micelles. The spectra of FSC micelles showed two endothermic melting peaks at 20.5 and 40.6 °C, which were ascribed to different crystalline phases of PCL in FSC micelles. FSC-16 micelles showed smaller endothermic melting peaks than FSC micelles, demonstrating that the encapsulation of hexadecanol hindered the crystallization process due to the copolymer/hexadecanol interactions. As shown in Figure 3b, there was around 20% of CPT release from FC-16 micelles at 0 and 10 mM GSH as well as from FSC-16 micelles at 0 and 2 μM GSH. The CPT release from FSC-16 micelles was accelerated to about 70% and 98% after incubation with 10 and 40 mM GSH for 100 h, respectively. These results showed that hexadecanol-included micelles still remained with good stability during circulation and in the extracellular space, and the reductive sensitivity of CPT release was significantly enhanced.

Reduction-Sensitive Destabilization of Micelles. The changes of micelle sizes and morphologies as well as the fluorescent intensity of pyrene in micelles were estimated after incubation with GSH. As shown in Figure 4a, there was no significant difference in the size of FC-16 micelles after incubation with 10 mM GSH for 48 h, but that of FSC-16

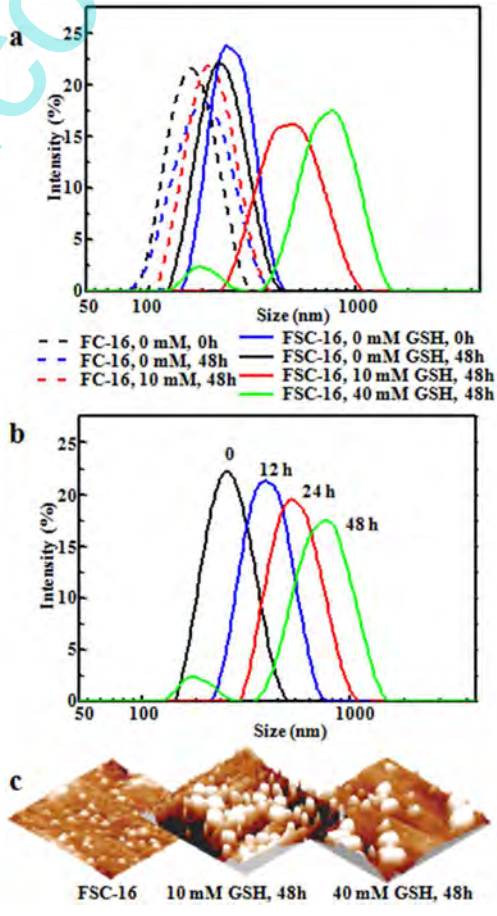

Figure 4. (a) Typical DLS images of FSC-16 micelles after incubation at 37 °C in PBS and PBS containing 2 μM and 10 and 40 mM GSH, compared with FC-16 micelles without disulfide linkage. (b) Typical DLS images of FSC-16 micelles after incubation at 37 °C in PBS containing 40 mM GSH for up to 48 h. (c) Typical AFM images of FSC-16 micelles and those after incubation in PBS containing 10 and 40 mM GSH for 48 h.

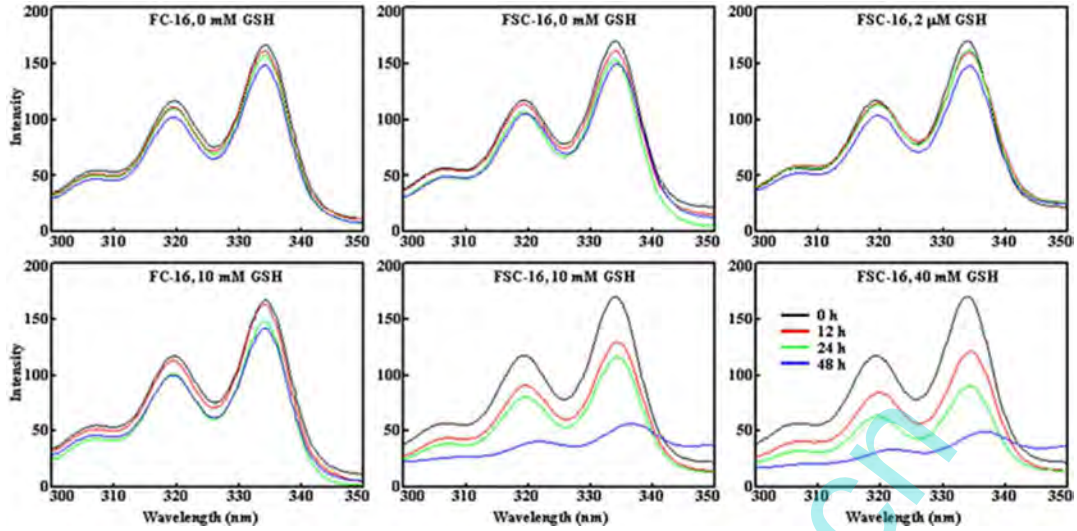

Figure 5. Fluorescence spectra of pyrene loaded in FSC-16 micelles after incubation at 37 °C in PBS and PBS containing 2 μM and 10 and 40 mM GSH, compared with FC-16 micelles without disulfide linkage.

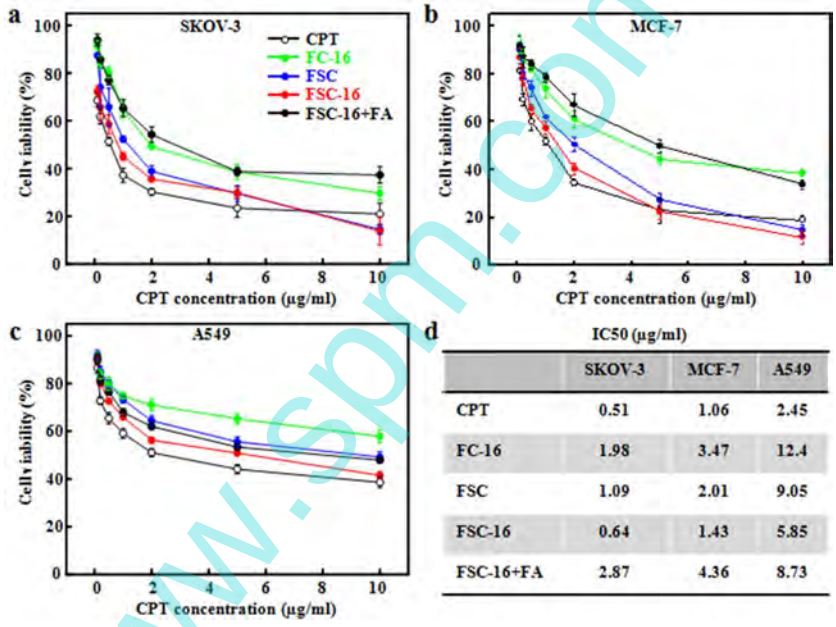

	SKOV-3	MCF-7	A549
CPT	0.51	1.06	2.45
FC-16	1.98	3.47	12.4
FSC	1.09	2.01	9.05
FSC-16	0.64	1.43	5.85
FSC-16+FA	2.87	4.36	8.73

Figure 6. (a) Cytotoxicity of free CPT, FC-16, FSC, FSC-16 micelles, and FSC-16 micelles with the inoculation of free FA (FSC-16+FA) to SKOV-3, (b) MCF-7, and (c) A549 cells after incubation for 72 h (n = 5). (d) IC_{50}s of CPT, FC-16, FSC, FSC-16, and FSC-16 + FA micelles against SKOV-3, MCF-7, and A549 cells.

micelles indicated an increase from around 200 nm to 360 and 700 nm with a broad distribution at 10 and 40 mM GSH, respectively. It should be noted that there was no significant change in the size and size distribution of FSC-16 micelles after incubation for 48 h in the absence of GSH, suggesting a good stability during circulation. As shown in Figure 4b, after incubation with 40 mM GSH, FSC-16 micelles indicated a significant increase in the average size, but a decrease in the intensity along with the incubation time. The disulfide linkages between PCL and CPT were broken in response to reductive GSH, and the changes in the hydrophilic/hydrophobic balance of matrix polymers led to an aggregation of micelles. Figure 4c shows typical AFM images of FSC-16 micelles after incubation with GSH for 48 h. Compared with that in the absence of GSH, FSC-16 micelles formed aggregates in an irregular shape and a larger size after incubation with 10 and 40 mM GSH.

The reductive sensitivity of FSC-16 micelles to GSH was also determined from the fluorescent intensity of pyrene loaded in micelles. The solubility of pyrene in water is very low, and the fluorescence is sensitive to the polarity of the surrounding environment. After dissociation of the micelles, a decrease in fluorescence intensities should be observed for pyrene, which was preferentially solubilized into hydrophobic cores of micelles.[25] Figure 5 summarizes the fluorescence intensities of pyrene-loaded micelles after incubation with different GSH levels. The fluorescence intensities of pyrene-loaded FC-16 micelles were nearly unchanged after incubation in the absence of GSH or with 10 mM GSH for 48 h. Compared with those in 2 μM GSH or in the absence of GSH, pyrene-loaded FSC-16

dx.doi.org/10.1021/mp500468d | Mol. Pharmaceutics 2014, 11, 4258−4269

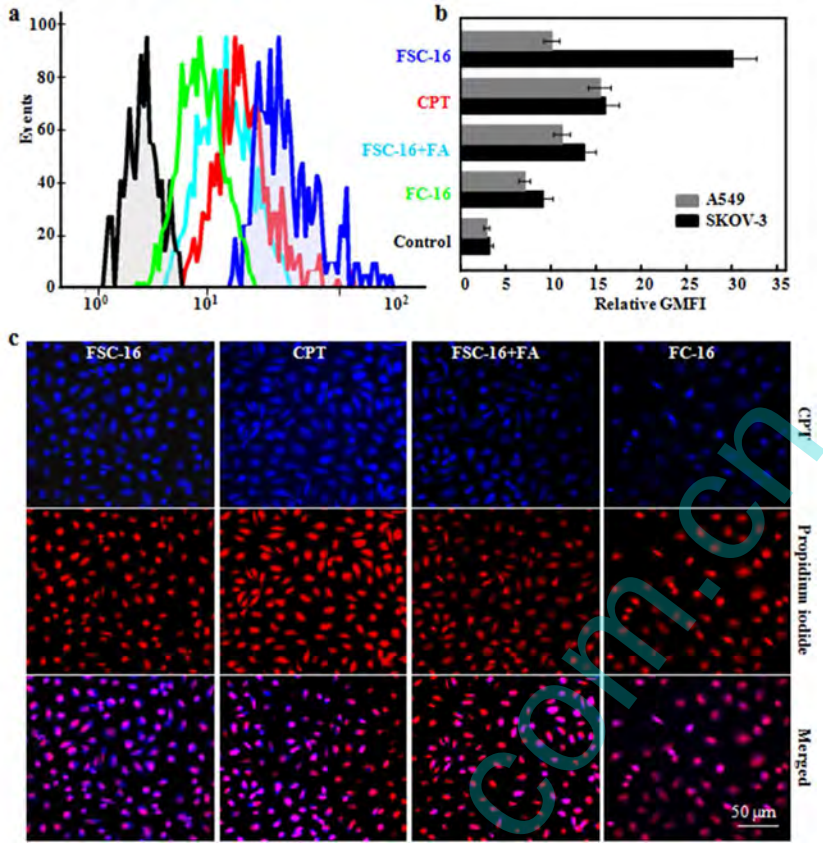

Figure 7. (a) Typical histogram of fluorescence intensities measured on SKOV-3 cells after incubation with free CPT, FC-16, FSC-16 micelles, and FSC-16 micelles with the inoculation of free FA (FSC-16 + FA). (b) Relative geometrical mean fluorescence intensity (GMFI) of SKOV-3 and A549 cells after treatment with free CPT, FC-16, FSC-16, and FSC-16 + FA micelles (n = 3). (c) Typical CLSM images of SKOV-3 cells, counterstained by PI, after incubation with free CPT, FC-16, FSC-16, and FSC-16 + FA micelles.

micelles indicated an obvious decrease in the fluorescence intensity after incubation in 10 and 40 mM GSH for 48 h, suggesting the gradual release of pyrene from FSC-16 micelles. Therefore, the above results verified that FSC-16 micelles could remain in good stability during circulation and in the extracellular space and display remarkable reductive sensitivity in response to GSH levels inside cells, which were suitable for intracellular delivery of anticancer drugs.[40]

***In Vitro* Cytotoxicity of Micelles.** In the current study, three types of tumor cells with different expression profiles of FA receptors were used for the cytotoxicity and cellular uptake tests of FC-16, FSC, and FSC-16 micelles. MCF-7 and SKOV-3 cells overexpress FA receptors on the surface, and SKOV-3 cells have stronger expressions than MCF-7, while FA receptors were rarely expressed on A549 cells.[41] Figure 6 shows the cell viability after incubation for 72 h, and the half maximal inhibitory concentration (IC_{50}) was determined to show the effectiveness to inhibit the growth of tumor cells (Figure 6d). The IC_{50} of free CPT was lower than those of micelle formulation, due to that CPT was available only after the breakdown of polymer−drug conjugates inside cells.[14] Compared with FC micelles, the inoculation of disulfide linkages in FSC micelles had a higher release rate of CPT, leading to lower IC_{50}s for all the three types of tumor cells. Similarly, higher CPT release from FSC-16 micelles indicated a lower IC_{50} than that of FSC micelles. However, the difference in IC_{50}s of FSC-16, FSC, and FC micelles were different among the tumor cells. As shown in Figure 6, FSC-16 micelles indicated an over 3-fold lower IC_{50} than FC micelles for SKOV-3 cells. The difference in IC_{50}s between FSC-16 and FC-16 was around 2-fold for A549 cells, while that for MCF-7 was set between those of SKOV-3 and A549 cells. Additionally, the IC_{50} of FSC-16 micelles for A549 cells was around 2-fold higher than that of free CPT, while the IC_{50}s of FSC-16 micelles and free CPT were very close for SKOV-3 cells. The cytotoxicity enhancement by the FA receptor-mediated uptake was further confirmed after interruption of the interactions by free FA. As shown in Figure 6, compared with A549 cells, there were remarkable increases in IC_{50}s for SKOV-3 and MCF-7 cells after the addition of free FA, due to the competitive binding of FA receptors and less effective uptake of FSC-16 micelles. Additionally, the effect of FA addition was more significant on SKOV-3 than that on MCF-7 cells, due to higher densities of FA receptors on SKOV-3 cells. Considering that an equivalent amount of CPT was dosed in the cell viability tests, the pronounced cytotoxicity of FSC-16 micelles relied on FA receptor-mediated cellular uptake and reduction-sensitive release of CPT.

Cellular Uptake and Intracellular CPT Release of Micelles. Because CPT is fluorescent, it can be used directly to measure its cellular uptake without introducing additional fluorescent probes. Figure 7a shows a typical histogram of fluorescence measured on SKOV-3 cells after incubation with either free CPT or CPT-loaded FSC-16 and FC-16 micelles. A lower fluorescence intensity was observed for FC-16 than FSC-16 micelles. Although there was no apparent shift for free CPT, the histogram of cells shifted to the direction of lower fluorescence intensity after the addition of free FA into the

media, suggesting that free FA prevented FSC-16 micelles from transporting into SKOV-3 cells by competitive binding to FA receptors on the cell surface. Figure 7b summarizes the relative geometrical mean fluorescence intensity (GMFI) of SKOV-3 and A549 cells after treatment with either FSC-16 or FC-16 micelles. The breakdown of reduction-sensitive linkages caused a rapid dissociation of FSC-16 micelles after cellular uptake, and the concentration gradient caused significantly higher cellular uptake efficiency than FC-16 micelles for both SKOV-3 and A549 cells ($p < 0.05$). When A549 cells were incubated with FSC-16 micelles, there was no significant difference in the cellular uptake regardless of the FA addition in the media ($p > 0.05$). However, when SKOV-3 cells were incubated with FSC-16 micelles, the inoculation of free FA led to a significant decrease in the relative GMFI from 30 to 13 ($p < 0.05$). Thus, the flow cytometry results directly demonstrated that FSC-16 micelles were transported within cells by an FA receptor-mediated endocytosis process.

The antitumor mechanism of CPT and its analogues are based on the inhibition of DNA replication and RNA transcription by stabilizing the cleavable complexes formed between topoisomerase I and DNA. The cellular uptake of micelles and the distribution of CPT released from FSC-16 micelles were observed by CLSM after nuclei staining by PI on SKOV-3 cells. As shown in Figure 7c, the blue fluorescence intensity of FSC-16 micelles was higher than that of FC-16 micelles and FSC-16 micelles with the treatment of free FA, indicating that the CLSM observation was in good agreement with the flow cytometry analysis. It should be noted that only CPT released from micelles can be distributed into nuclei; so, the localization of CPT released from micelles within the cells was studied by using the blue fluorescence from CPT and the red fluorescence from PI staining. As shown in Figure 7c, the majority of blue fluorescent signals were concentrated in the nuclei, and the overlay of the two fluorescence images showed purple spots. As expected, the majority of CPT signals in the cells treated with free CPT clearly overlapped with PI-stained nuclei. Compared with FC-16 micelles, a stronger blue fluorescence of CPT was observed in the nuclei of cells treated with FSC-16 micelles, indicating that the degradation of GSH-responsive disulfide linkages accelerated the intracellular CPT release from FSC-16 micelles.

Cell Apoptosis after Treatment with Micelles. Annexin V-FITC/PI staining was used to quantify the percentages of apoptotic cells induced by different micelle formulations. As shown in Figure 8, FSC-16 micelles induced the most significant apoptosis, and the percentage of total apoptotic cells, including early and late apoptotic cells, was comparable with that of free CPT at around 50%. A slower release of CPT from FSC micelles led to a decrease in the percentage of total apoptotic cells to 39.8 ± 3.5%. The lower release of CPT from FC-16 micelles indicated an even lower apoptosis rate at 32.3 ± 2.8%. Additionally, the less significant cellular uptake of FSC-16 micelles after the addition of free FA into the media resulted in a significant decrease in the percentage of apoptotic cells to 30.7 ± 3.0%. It was suggested that the FA receptor mediated uptake and reduction-sensitive release of CPT from FSC-16 micelles led to the significant cytotoxicity and cell apoptosis.

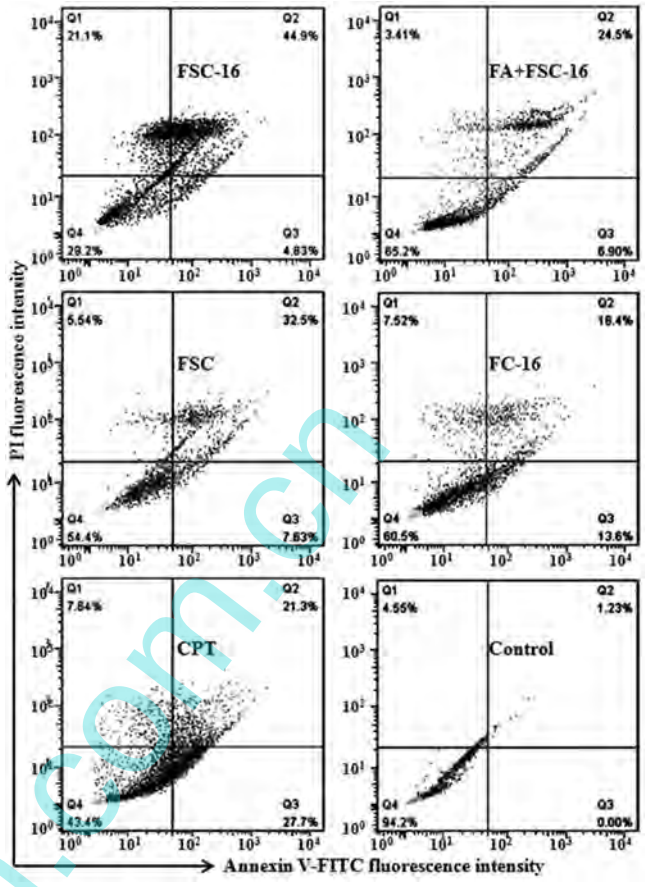

Figure 8. (a) Flow cytometry analysis of cell apoptosis after incubation of SKOV-3 cells with free CPT, FSC-16, FSC, FC-16 micelles, and FSC-16 micelles with the inoculation of free FA (FSC-16 + FA) for 48 h, compared with no treatment as control. Lower left of each image, living cells; lower right, early apoptotic cells; upper right, late apoptotic cells; upper left, necrotic cells. Inserted numbers in each area indicate the percentage of cells present in this area.

CONCLUSIONS

FA-decorated polymer−CPT conjugates were synthesized with disulfide linkages between CPT and amphiphilic PECL copolymers. After the addition of hexadecanol during micelle formation, FSC-16 micelles were obtained with a low CMC of around 2 μg/mL, and the conjugated CPT was rapidly released out in response to intracellular levels of GSH. The reductive sensitivity was also confirmed from the changes of micelle sizes and morphologies as well as the fluorescent intensity of pyrene loaded in micelles. Through comparing the behaviors of SKOV-3, MCF-7, and A549 cells after micelle treatment, the most significant cytotoxicity and cell apoptosis of FSC-16 micelles were demonstrated to be resulted from the FA receptor mediated uptake and reduction-sensitive release of CPT. CLSM observations indicated that CPT was distributed into nuclei after cellular uptake and intracellular release from FSC-16 micelles. Thus, through designing amphiphilic copolymers containing reduction-sensitive linkages between CPT and polymers, optimizing the micellization process with hexadecanol inoculation, and providing FA as targeting moieties, the polymer−drug conjugate micelles show advantages in inhibiting premature release during circulation, enhancing the cellular uptake at the tumor tissues, and promoting the intracellular release and nuclei location of the active moieties.

■ ASSOCIATED CONTENT

Supporting Information

Synthesis procedure of FC copolymer and their NMR spectra; the ^{1}H NMR and DSC characterization of micelles and their CMC determinations were included. This material is available free of charge via the Internet at http://pubs.acs.org.

■ AUTHOR INFORMATION

Corresponding Author

*Phone: +8628-87634068. Fax: +8628-87634649. E-mail: xhli@swjtu.edu.cn.

Author Contributions

†The authors contributed equally to this work.

Notes

The authors declare no competing financial interest.

■ ACKNOWLEDGMENTS

This work was supported by National Natural Science Foundation of China (21274117), Specialized Research Fund for the Doctoral Program of Higher Education (20120184110004), Scientific and Technical Supporting Programs of Sichuan Province (2013SZ0084), and Construction Program for Innovative Research Team of University in Sichuan Province (14TD0050).

■ REFERENCES

(1) Deng, C.; Jiang, Y.; Cheng, R.; Meng, F.; Zhong, Z. Biodegradable polymeric micelles for targeted and controlled anticancer drug delivery: Promises, progress and prospects. *Nano Today* **2012**, *7* (5), 467−480.

(2) Hrkach, J.; Hoff, D. V.; Ali, M. M.; Andrianova, E.; Auer, J.; Campbell, T.; Witt, D. D.; Figa, M.; Figueiredo, M.; Horhota, A.; Low, S.; Mcdonnell, K.; Peeke, E.; Retnarajan, B.; Sabnis, A.; Schnipper, E.; Song, J. J.; Song, Y. H.; Summa, J.; Tompsett, D.; Troiano, G.; Hoven, T. V. G.; Wright, J.; Lorusso, P.; Kantoff, P. W.; Bander, N. H.; Sweeney, C.; Farokhzad, O. C.; Langer, R.; Zale, S. Preclinical development and clinical translation of a PSMA-targeted docetaxel nanoparticle with a differentiated pharmacological profile. *Sci. Transl. Med.* **2012**, *4* (128), 128ra39.

(3) Shuai, X.; Ai, H.; Nasongkla, N.; Kim, S.; Gao, J. Micellar carriers based on block copolymers of poly(ε-caprolactone) and poly(ethylene glycol) for doxorubicin delivery. *J. Controlled Release* **2004**, *98* (3), 415−426.

(4) Wang, W.; Sun, H.; Meng, F.; Ma, S.; Liu, H.; Zhong, Z. Precise control of intracellular drug release and anti-tumor activity of biodegradable micellar drugs via reduction-sensitive shell-shedding. *Soft Matter* **2012**, *8* (14), 3949−3956.

(5) Fleige, E.; Quadir, M. A.; Haag, R. Stimuli-responsive polymeric nanocarriers for the controlled transport of active compounds: Concepts and applications. *Adv. Drug Delivery Rev.* **2012**, *64* (9), 866−884.

(6) Muthu, M. S.; Rajesh, C. V.; Mishra, A.; Singh, S. Stimulus-responsive targeted nanomicelles for effective cancer therapy. *Nanomedicine* **2009**, *4* (6), 657−667.

(7) Lee, S. Y.; Kim, S.; Tyler, J. Y.; Park, K.; Cheng, J. X. Blood-stable, tumor-adaptable disulfide bonded mPEG-(Cys)4-PDLLA micelles for chemotherapy. *Biomaterials* **2013**, *34* (2), 552−561.

(8) Wei, H.; Zhuo, R. X.; Zhang, X. Z. Design and development of polymeric micelles with cleavable links for intracellular drug delivery. *Prog. Polym. Sci.* **2013**, *38* (3), 503−535.

(9) Andresen, T. L.; Jensen, S. S.; Jørgensen, K. Advanced strategies in liposomal cancer therapy: Problems and prospects of active and tumor specific drug release. *Prog. Lipid Res.* **2005**, *44* (1), 68−97.

(10) Torchilin, V. Tumor delivery of macromolecular drugs based on the EPR effect. *Adv. Drug Delivery Rev.* **2011**, *63* (3), 131−135.

(11) van Nostrum, C. F. Covalently cross-linked amphiphilic block copolymer micelles. *Soft Matter* **2011**, *7* (7), 3246−3259.

(12) Bütün, V.; Wang, X. S.; de Paz Banez, M. V.; Robinson, K. L.; Billingham, N. C.; Armes, S. P. Synthesis of shell cross-linked micelles at high solids in aqueous media. *Macromolecules* **2000**, *33* (1), 1−3.

(13) Wang, K.; Liu, Y.; Yi, W. J.; Li, C.; Li, Y. Y.; Zhuo, R. X.; Zhang, X. Z. Novel shell-cross-linked micelles with detachable PEG corona for glutathione-mediated intracellular drug delivery. *Soft Matter* **2013**, *9* (3), 692−699.

(14) Hu, X.; Jing, X. Biodegradable amphiphilic polymer−drug conjugate micelles. *Expert Opin. Drug Delivery* **2009**, *6* (10), 1079−1090.

(15) Mi, Z.; Burke, T. G. Differential interactions of camptothecin lactone and carboxylate forms with human blood components. *Biochemistry* **1994**, *33* (34), 10325−10336.

(16) Larson, N.; Ghandehari, H. Polymeric conjugates for drug delivery. *Chem. Mater.* **2012**, *24* (5), 840−853.

(17) Paranjpe, P. V.; Chen, Y.; Kholodovych, V.; Welsh, W.; Stein, S.; Sinko, P. J. Tumor-targeted bioconjugate based delivery of camptothecin: Design, synthesis and in vitro evaluation. *J. Controlled Release* **2004**, *100* (2), 275−292.

(18) Zhang, W.; Huang, J.; Fan, N.; Yu, J.; Liu, Y.; Liu, S.; Wang, D.; Li, Y. Nanomicelle with long-term circulation and enhanced stability of camptothecin based on mPEGylated α,β-poly(l-aspartic acid)-camptothecin conjugate. *Colloids Surf., B* **2010**, *81* (1), 297−303.

(19) Fan, H.; Huang, J.; Li, Y.; Yu, J.; Chen, J. Fabrication of reduction-degradable micelle based on disulfide-linked graft copolymer-camptothecin conjugate for enhancing solubility and stability of camptothecin. *Polymer* **2010**, *51* (22), 5107−5114.

(20) Li, X. Q.; Wen, H. Y.; Dong, H. Q.; Xue, W. M.; Pauletti, G. M.; Cai, X. J.; Xia, W. J.; Shi, D. L.; Li, Y. Y. Self-assembling nanomicelles of a novel camptothecin prodrug engineered with a redox-responsive release mechanism. *Chem. Commun.* **2011**, *47* (30), 8647−8649.

(21) Lu, Y.; Low, P. S. Folate-mediated delivery of macromolecular anticancer therapeutic agents. *Adv. Drug Delivery Rev.* **2002**, *54* (5), 675−693.

(22) Hiki, S.; Kataoka, K. Versatile and selective synthesis of "click chemistry" compatible heterobifunctional poly(ethylene glycol)s possessing azide and alkyne functionalities. *Bioconjugate Chem.* **2010**, *21* (2), 248−254.

(23) Tyrrell, Z. L.; Shen, Y. Q.; Radosz, M. Fabrication of micellar nanoparticles for drug delivery through the self-assembly of block copolymers. *Prog. Polym. Sci.* **2010**, *35* (9), 1128−1143.

(24) Wilhelm, M.; Zhao, C. L.; Wang, Y.; Xu, R.; Winnik, M. A.; Mura, J. L.; Riess, G.; Croucher, M. D. Poly(styrene-ethylene oxide) block copolymer micelle formation in water: A fluorescence probe study. *Macromolecules* **1991**, *24* (5), 1033−1040.

(25) Thambi, T.; Saravanakumar, G.; Chu, J. U.; Heo, R.; Ko, H.; Deepagan, V. G.; Kim, J. H.; Park, H. Synthesis and physicochemical characterization of reduction-sensitive block copolymer for intracellular delivery of doxorubicin. *Macromol. Res.* **2013**, *21* (1), 100−107.

(26) Chen, Z.; Cai, X.; Yang, Y.; Wu, G.; Liu, Y.; Chen, F.; Li, X. Promoted transfection efficiency of pDNA polyplexes-loaded biodegradable microparticles containing acid-labile segments and galactose grafts. *Pharm. Res.* **2012**, *29* (2), 471−482.

(27) Venditto, V. J.; Simanek, E. E. Cancer therapies utilizing the camptothecins: A review of the *in vivo* literature. *Mol. Pharmaceutics* **2010**, *7* (2), 307−349.

(28) Wang, Y. J.; Gou, M. L.; Gong, C. Y.; Wang, C.; Qian, Z. Y.; Feng, L. Y.; Luo, F. Pharmacokinetics and disposition of nanomedicine using biodegradable PEG/PCL polymers as drug carriers. *Curr. Drug Metab.* **2012**, *13* (4), 338−353.

(29) Zhu, Y.; Gao, C.; Liu, X.; He, T.; Shen, J. Immobilization of biomacromolecules onto aminolyzed poly(L-lactic acid) toward acceleration of endothelium regeneration. *Tissue Eng.* **2004**, *10* (1−2), 53−61.

(30) Jia, L.; Li, Z.; Zhang, D.; Zhang, Q.; Shen, J.; Guo, H.; Tian, X.; Liu, G.; Zheng, D.; Qi, L. Redox-responsive catiomer based on PEG-

ss-chitosan oligosaccharide-ss-polyethylenimine copolymer for effective gene delivery. *Polym. Chem.* **2012**, *4* (1), 156−165.
(31) Shen, Y.; Jin, E.; Zhang, B.; Murphy, C. J.; Sui, M.; Zhao, J.; Wang, J.; Tang, J.; Fan, M.; Kirk, E. V.; Murdoch, W. J. Prodrugs forming high drug loading multifunctional nanocapsules for intracellular cancer drug delivery. *J. Am. Chem. Soc.* **2010**, *132* (12), 4259−4265.
(32) Basile, L.; Pignatello, R.; Passirani, C. Active targeting strategies for anticancer drug nanocarriers. *Curr. Drug Delivery* **2012**, *9* (3), 255−268.
(33) Heald, C. R.; Stolnik, S.; Kujawinski, K. S.; Matteis, C. D.; Garnett, M. C.; Iiium, L.; Davis, S. S.; Purkiss, S. C.; Barlow, R. J.; Gellert, P. R. Poly(lactic acid)-poly(ethylene oxide) (PLA-PEG) nanoparticles: NMR studies of the central solid-like PLA core and the liquid PEG corona. *Langmuir* **2002**, *18* (9), 3669−3675.
(34) Bae, Y. H.; Park, K. Targeted drug delivery to tumors: myths, reality and possibility. *J. Controlled Release* **2011**, *153* (3), 198−205.
(35) Kong, M.; Park, H.; Cheng, X.; Chen, X. Spatial−temporal event adaptive characteristics of nanocarrier drug delivery in cancer therapy. *J. Controlled Release* **2013**, *172* (1), 281−291.
(36) Mu, L.; Feng, S. S. Vitamin E TPGS used as emulsifier in the solvent evaporation/extraction technique for fabrication of polymeric nanospheres for controlled release of paclitaxel (Taxol). *J. Controlled Release* **2002**, *80* (1), 129−44.
(37) Kuppusamy, P.; Li, H.; Ilangovan, G.; Cardounel, A. J.; Zweier, J. L.; Yamada, K.; Krishna, M. C.; Mitchell, J. B. Noninvasive imaging of tumor redox status and its modification by tissue glutathione levels. *Cancer Res.* **2002**, *62* (1), 307−312.
(38) Sun, H.; Guo, B.; Cheng, R.; Meng, F.; Liu, H.; Zhong, Z. Biodegradable micelles with sheddable poly(ethylene glycol) shells for triggered intracellular release of doxorubicin. *Biomaterials* **2009**, *30* (31), 6358−6366.
(39) Wong, A. D.; DeWit, M. A.; Gillies, E. R. Amplified release through the stimulus triggered degradation of self-immolative oligomers, dendrimers, and linear polymers. *Adv. Drug Delivery Rev.* **2012**, *64* (11), 1031−1045.
(40) Yan, L.; Wu, W.; Zhao, W.; Qi, R.; Cui, D.; Xie, Z.; Huang, Y.; Tong, T.; Jing, X. Reduction-sensitive core-cross-linked mPEG−poly(ester-carbonate) micelles for glutathione-triggered intracellular drug release. *Polym. Chem.* **2012**, *3* (9), 2403−2412.
(41) Miotti, S.; Bagnoli, M.; Ottone, F.; Tomassetti, A.; Colnaghi, M. I.; Canevari, S. Simultaneous activity of two different mechanisms of folate transport in ovarian carcinoma cell lines. *J. Cell. Biochem.* **1997**, *65* (4), 479−491.